

УДК 539.1.074.3

THE «MINISKIRT» COUNTER ARRAY AT CDF II

A. Artikov^a, *G. Bellettini*^b, *J. Budagov*^a, *F. Cervelli*^b,
I. Chirikov-Zorin^a, *G. Chlachidze*^a, *D. Chokheli*^a, *D. Dreossi*^c,
M. Incagli^b, *A. Menzione*^b, *G. Pauletta*^d, *A. Penzo*^c,
O. Pukhov^a, *A. Scribano*^b, *A. Stefanini*^b

^a Joint Institute for Nuclear Research, Dubna^b INFN, Pisa, Italy^c INFN, Trieste, Italy^d INFN and University of Udine, Italy

Muon detection is fundamental to many of the most interesting analyses at CDF II. For more efficient muon registration in Run II it was decided to increase geometrical coverage. The so-called «miniskirt» counters are part of this upgrade. The original design parameters of the «miniskirt» and mixed «miniskirt» scintillation counters for the CDF Muon System are presented. The modifications, testing and installation of these counters within the CDF Upgrade Project are described in detail. The timing characteristics of mixed «miniskirt» counters are also investigated using cosmic muons. The measurements show that the time resolution does not exceed 2.2 ns.

Регистрация мюонов является одной из важнейших задач для большинства экспериментов на CDF II. Для более эффективной регистрации мюонов в Run II было предусмотрено увеличение площади покрытия установки сцинтиляционными счетчиками. Так называемые «miniskirt»-счетчики являются частью этого плана. В статье представлены конструкция и размеры мюонных сцинтиляционных счетчиков «miniskirt» и комбинированных «miniskirt». В деталях описаны модернизация, сборка, тестирование и установка этих счетчиков на CDF II. Также приведены временные характеристики комбинированных «miniskirt»-счетчиков, измеренные при регистрации космических мюонов. Измерения показали, что временное разрешение этих счетчиков не хуже 2,2 нс.

INTRODUCTION

Muon detection is fundamental to many of the most interesting analyses at CDF. In the course of Run II, the collaboration expects to collect hundreds of $t\bar{t}$ decays yielding a muon as well as several million B -hadron events involving $J/\psi \rightarrow \mu^+\mu^-$ decays. Muon detection is also of fundamental importance in the study of W -boson properties and in the search for Higgs production associated with W or Z bosons [1]. Considerable effort therefore went into extending the muon detector coverage for Run II, which started in March 2001.

The CDF II muon detector system consists of multiple layers of drift chambers and scintillation counters, which span the pseudorapidity ($|\eta|$) range between 0 and 1.5. Detectors spanning different ranges have different geometries, and the muon scintillation counter system includes subsystems in the regions that have come to be known as the «central» ($0 < |\eta| < 0.6$), «extended» ($0.6 < |\eta| < 1.2$) and «intermediate» ($1.2 < |\eta| < 1.5$) regions of the

detector. During Run I, the «extended» region (referred to as the CMX) spanned two thirds of the azimuthal acceptance with eight layers of drift tubes sandwiched between two layers of scintillation counters (known as the CSX) [2]. Though much of the missing 90° of the azimuthal coverage, on both the east and west sides of the detector, were constructed before Run I, installation was delayed until the «CDF Upgrade» and, at that time, it was found necessary to introduce several modifications to the original design. These subsystems of the CMX came to be known as the «miniskirts», because they covered the lower section of the azimuthal range. The counters (which we refer to collectively as the MSX) of one of these «miniskirts» are illustrated in Fig. 1.

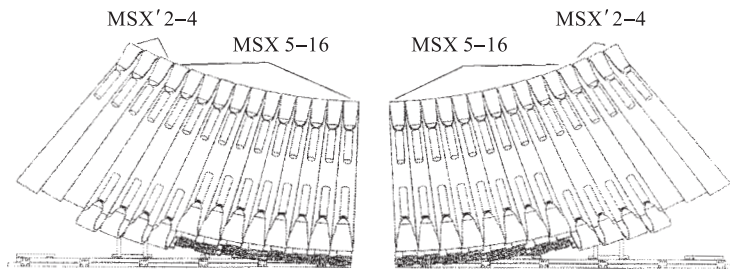


Fig. 1. The scheme of «miniskirt» counters arrangement. There are 24 standard (MSX) and 6 mixed (MSX') counters on each side of CDF

In this note we recall the original design parameters and describe in detail the modifications, testing and installation of the MSX counters as part of the CDF Upgrade Project.

1. DESIGN PARAMETERS

Like the CSX, the MSX are trapezoidal counters constructed from NE114 scintillator, produced about 10 years ago by Nuclear Enterprises. However, the MSX are 15 mm thick (as opposed to the CSX, which are 20 mm thick) and the scintillator which is apparently of superior quality in that it has not yet shown any evidence of the premature aging which has shown up in the central counters (known as the CSPs) and the CSX [2, 3]. The dimensions of the CSX and MSX are shown in Figs. 2–4.

The CSX [2] counters sandwich the drift chambers, as shown in Fig. 2. The «internal» (i. e., those closest to the interaction point) and the «external» counters are read out of opposite sides so as to allow the timing uncertainty associated with hit position to be eliminated by the application of «mean timing» [2]. Due to space restrictions the MSX cover only one side (that closest to the interaction point) of the «miniskirts» and, in order to retain the ability to do «mean timing», the counters were designed to be read out of both ends, through curved Lucite light guides coupled to 5.1-cm-diameter EMI 9814B photomultipliers (PMTs), as illustrated in Fig. 3 (these PMTs are now produced by Electron Tubes Inc., UK).

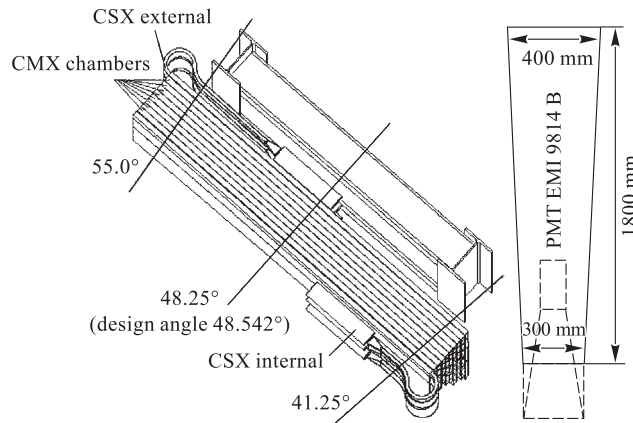
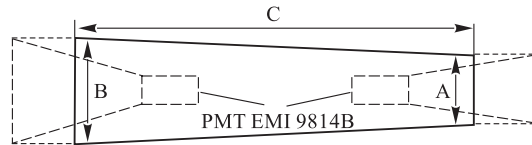


Fig. 2. A CMX section showing how the CSX counters sandwich the chambers between them. CSX dimensions are also shown



MSX	5	6	7	8	9	10	11	12	13	14	15	16
A	171.2	169.2	167.2	165.7	164.2	162.7	161.2	160.2	159.2	158.7	158.2	157.7
B	243.3	239.3	235.8	232.8	229.8	227.3	224.8	223.2	221.8	220.3	219.3	218.8
C	1773.3	1747.3	1723.9	1703.0	1684.4	1668.0	1653.8	1641.5	1631.2	1622.7	1616.0	161.1

Fig. 3. Standard «miniskirt» (MSX) counters and their dimensions (in millimetres)

However, due to space restrictions, not foreseen in the original design, the curved Lucite light guides on one side of four of the counters on each side of either of the two «miniskirts» (referred to here as the mixed «miniskirts» or MSX') could not be accommodated (see Fig. 1). Conventional readout was therefore substituted by wavelength-shifter (WLS) fiber readout, as illustrated in Fig. 4. The WLS fibers (1-mm-diameter Y11 (200 ppm) fiber produced by Kuraray) were assembled into 15-fiber ribbons, which were glued (using BC-600 optical cement) to one of the long edges of the scintillators and read out by means of Hamamatsu H5783 photosensor, which incorporates new ultra compact photomultiplier R5600. Light collection was augmented by «mirroring» the end of the fibers furthest from the PMT photocathode. «Mirroring» was obtained by evaporating an aluminium coating on the polished ends of individual fibers. Reflection coefficients ranging between 70 and 90 % were obtained in this manner.

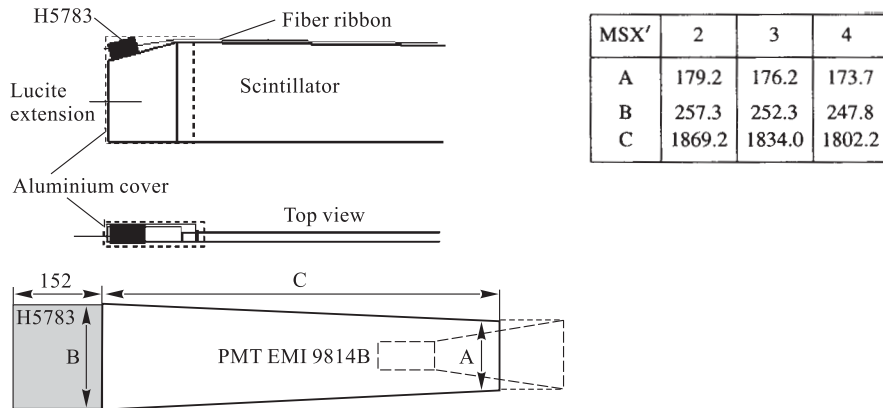


Fig. 4. Mixed «miniskirt» (MSX') counters and their dimensions (in millimetres). The mounting scheme for the H5783 on the broader end of the detector is also illustrated

This solution was arrived at after preliminary studies of the mean timing resolution. Issues related to time resolution are discussed in section 4.

2. COUNTER CALIBRATIONS AND PERFORMANCE PARAMETERS

Phototubes were «calibrated» by illuminating them with low-level light pulses from a fast blue LED (MICHIA NSPB310A), as illustrated schematically in Fig. 5, and isolating the peak corresponding to the single photoelectron according to a procedure similar to that described in [4]. As a result of this procedure, the calibration constant k (in channels/photoelectron), corresponding to the specific combination of PMT and ADC, and the PMT gain are extracted. These parameters as well as the average number of photoelectrons μ , used for the calibration, the HV at which the calibration was performed, and the noise rate at that HV were measured for 36 units of older EMI PMTs. They were used to select 20 of these older PMTs for low noise, high gain and, for counters with light guide readout on both sides, similar characteristics (the remaining 50 PMTs were new).

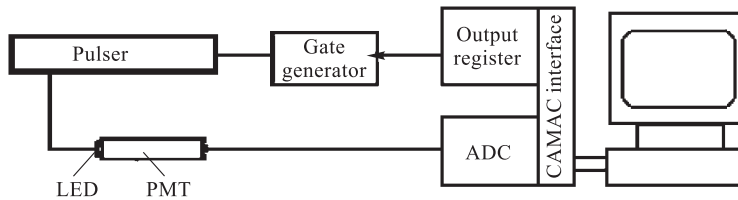


Fig. 5. Schematic representation of the calibration stand used for measuring the characteristics of PMTs

After calibration and assembly, the number of photoelectrons n_{pe} at the photocathode, corresponding to the passage of a cosmic muon, which we refer to here as the «counter sensitivity», was measured for all counters. These were obtained from the ADC measurements of the integrated signals as follows:

$$n_{pe} = \frac{\bar{Q} - Q_0}{k/A},$$

where \bar{Q} is the mean of the ADC output distribution; Q_0 is the pedestal; k is the calibration constant (in channels/photoelectron) for the specific combination of PMT and ADC, and A is the amplification factor necessary to view the single photoelectron peak while calibrating. A typical light yield distribution corresponding to cosmic muons is shown in Fig. 6. On the average, the «counter sensitivity» is ~ 80 photoelectrons/muon.

The characteristics of all MSX counters (operating plateau voltages and dark currents at those voltages, noise rates corresponding to 15-mV discriminator settings) were measured on the bench, prior to installation, using cosmic muons.

3. COUNTER ASSEMBLY

All counters were wrapped with diffuse, 127- μm -thick, aluminized paper reflector and a combination of 381- μm -thick black PVC sheet and 178- μm -thick black electrical tape. Single sheets of the reflector and the black PVC sheet were successively laid on all flat scintillator faces, which were then taped down at the edges so the overall thickness of the wrapping material covering the scintillator was 1.4 mm except for ~ 1.3 cm along the edges where the electric tape overlapped the PVC sheet.

All 5.1-cm PMTs were coupled to their light guides using standard CERN mounting assemblies for the EMI 9814B PMT, and surrounded by 0.5-mm-thick mu-metal and 1-cm-thick iron shields. The smaller Hamamatsu tubes were coupled to the polished ends of the fiber ribbons via Lucite adapter and mounted to Lucite extensions of the counters, as shown in Fig. 4. They were then surrounded by an aluminum light shield, which was taped down to the Lucite extension with black electrical tape. All PMTs were air-coupled to their respective light guides/adapters.

4. TIMING CONSIDERATIONS

Given the length of the scintillators, which generally ranges between ~ 160 and ~ 180 cm, and the average speed of light in the scintillator (~ 15 cm/ns), the uncertainty in the time at

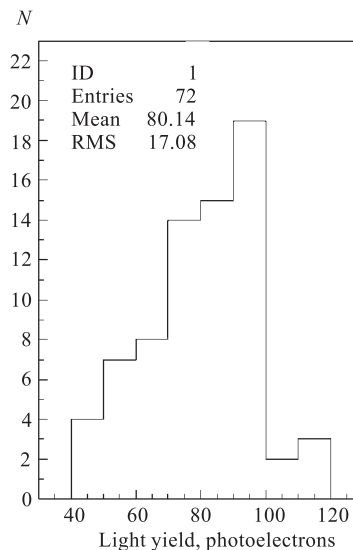


Fig. 6. The distribution of photoelectrons corresponding to a muon crossing the center of a «miniskirt» counter

which a muon reaches the counter ranges between ~ 10 and ~ 12 ns. This is comparable to the difference between the time a muon takes to reach the counters from the interaction point and the time a background muon takes to reach the same counters from the beam pipe upstream of the detector, at some point close to the MSX like, say, the entry point to the plug calorimeters. During Run I, the background of this type [2] would have overwhelmed the CSX signal had it not been for the introduction of a mean timer (MT) circuit, described in Ref. 2, to eliminate this uncertainty. Although the geometry around the beam pipe, on both sides of the detector has changed radically since Run I, particularly as regards the additional shielding (two concentric rings of 45.7-cm-thick steel, known as the snout and 61 cm donut between the beam pipe and the CSX and MSX counters [1]), introduced to reduce background, the acceptance of the plug calorimeters at low P_t has been increased, with a corresponding increase of material close to the beam pipe, and additional material in the form of small P_t calorimeters (known as the miniplugs) has been added upstream of the plug calorimeters. Therefore, we estimated the worst acceptable timing resolution from the MSX to be a standard deviation $\sigma = 3$ ns, which was sufficient to extract the signal from the background during Run I [2].

Mean timing is based on the assumption that the two ends of the detector are symmetrical. Under these conditions, if the time t_a at which the signal is emitted from the PMT at one end of the detector is $t + x$, where x is the distance (in nanoseconds) from the muon hit to that end of the detector, then the corresponding time t_b from the other side of the detector will be $t + l - x$, where l is the length (in nanoseconds) of the detector. The mean of these times then differs from the hit time t by a constant and a statistical fluctuation, which is determined by the combined fluctuations in the number of photoelectrons (n_{pe}) at the PMT photocathodes and by the multiplication statistics in the PMTs. If the counter is not symmetrical, a systematic uncertainty can also be expected to contribute to the total uncertainty.

Trapezoidal counters are not symmetrical and the MSX' counters, which are read out through a conventional light guide on the one end and via a WLS fiber ribbon on the other, are much less so. One might therefore expect a significant systematic contribution from this asymmetry to the overall σ . Furthermore, because the n_{pe} for WLS fiber readout is smaller than for conventional readout, we can also expect an increase in the statistical contribution to the overall uncertainty. Our first concern, before adopting this solution, was therefore to ascertain that the mean timing resolution obtained under these conditions was adequate.

4.1. Preliminary Tests. The first tests were performed in a nondestructive manner by leaving the Lucite light guides on both ends of an MSX counter and optically coupling a WLS fiber ribbon to one edge by means of optical grease. Both the light guides were read out by means of EMI 9814B PMTs, whereas the two ends of the WLS ribbon were read out by Hamamatsu R4125 PMTs (see Figs. 7, 8). By combining different readouts one could investigate how the corresponding asymmetry contributed to each resulting mean time. For this investigation, the statistical contribution was reduced by using a relatively high-intensity pulsed (5 ns half-width) UV laser (LN300 pulsed nitrogen laser with a spectral output of 337.1 nm, pulse width of 300 ps, energy stability of 5%) to illuminate the scintillator at localized positions corresponding to 2-mm-diameter holes in the 25.4- μ m black PVC sheet used to wrap the scintillator (see Figs. 7, 8).

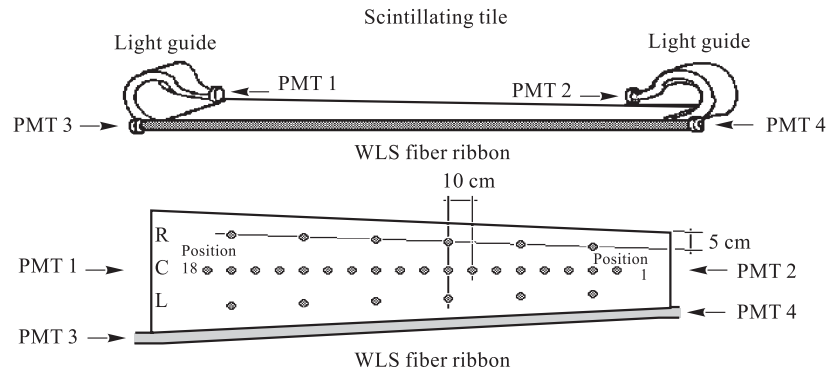


Fig. 7. Counter layout for the preliminary timing tests, showing the fiber ribbon and the location of holes in the wrapping through which the scintillator was excited with a pulsed UV laser

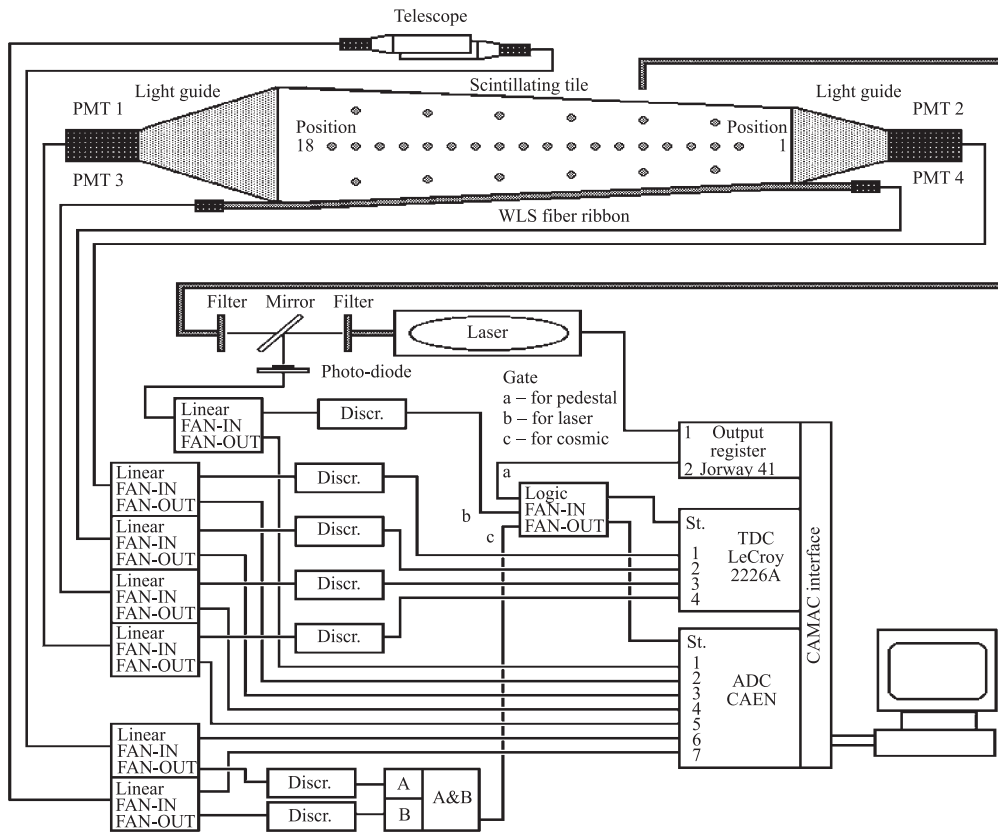


Fig. 8. The corresponding data acquisition electronics and readout scheme

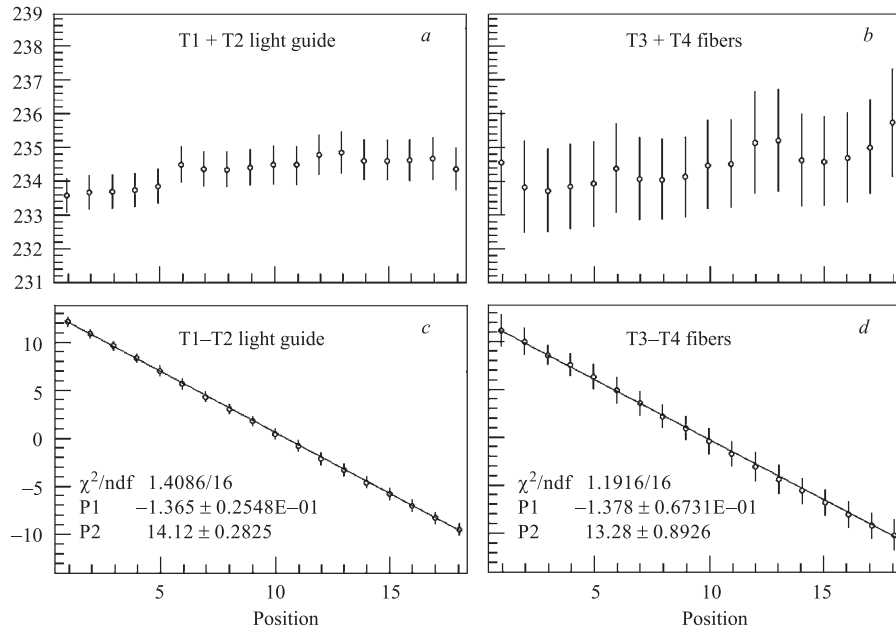


Fig. 9. Sums and differences of TDC outputs for similar readouts (light guides in plots *a*, *c* and fibers in plots *b*, *d*) (in nanoseconds)

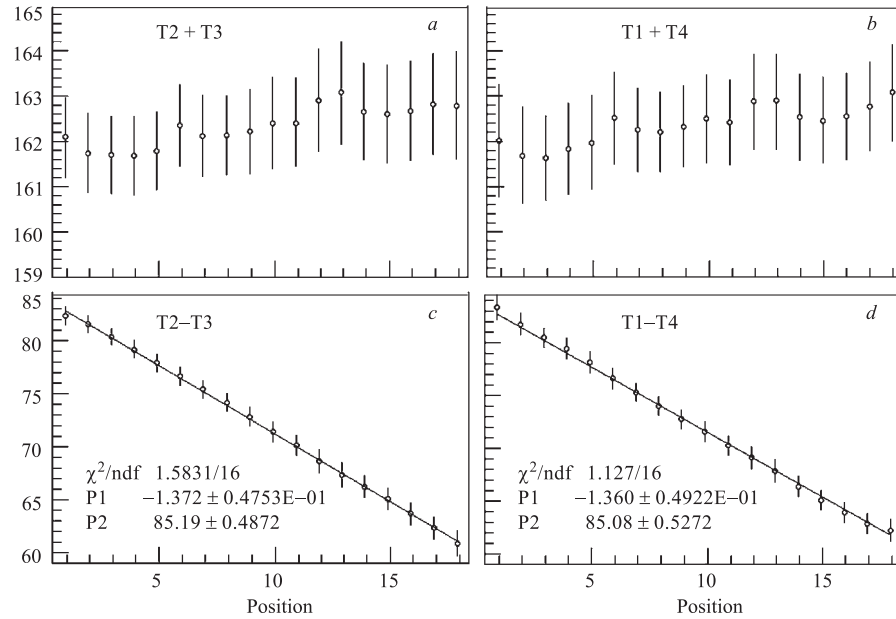


Fig. 10. Similar measurements for dissimilar readouts (in nanoseconds)

The outputs of each of the four PMTs were discriminated and used to stop TDCs, which had been started by the laser trigger. Sums and differences of pairs of TDCs corresponding to similar readouts are plotted in Fig.9 as a function of position along the long dimension of the counter (the distance between two neighbouring hole positions is 10 cm, as shown in Fig. 7). The effective velocity of the light in the scintillator and the WLS fiber were calculated from the differences and found to be (14.6 ± 0.3) cm/ns and (14.5 ± 0.7) cm/ns, respectively. The sums of these outputs correspond to the mean times. Ideally, they should be constant but Fig.9 shows significant variations. In the case of light guides readout, a variation of ~ 0.5 ns is observed between the two ends of the counter. However, the variation is not linear with displacement from one end and it reaches a maximum of ~ 1 ns at $\sim 1/3$ of the distance from the wider end of the counter. These variations are attributed to a combination of the trapezoidal shape of the counter and the increase of light acceptance as the light source approaches the light guide. The statistical uncertainties are about 0.5 ns and, apart from the factors already mentioned in the previous section (fluctuations in the number of photoelectrons at the PMT photocathodes and multiplication statistics in the PMTs), are determined also by fluctuations in light collection and in triggering time of the discriminator.

The maximum deviation in the mean times calculated from the two WLS fiber outputs is similar (~ 1 ns) but it appears, as might be expected, to be approximately linear with displacement along the counter. Statistical uncertainties are considerably larger in this latter case because of the smaller light collection efficiency.

Systematics related to the displacement of the light source in the direction transverse to the longer dimension, i. e., across the detector, were also investigated and found to be negligible

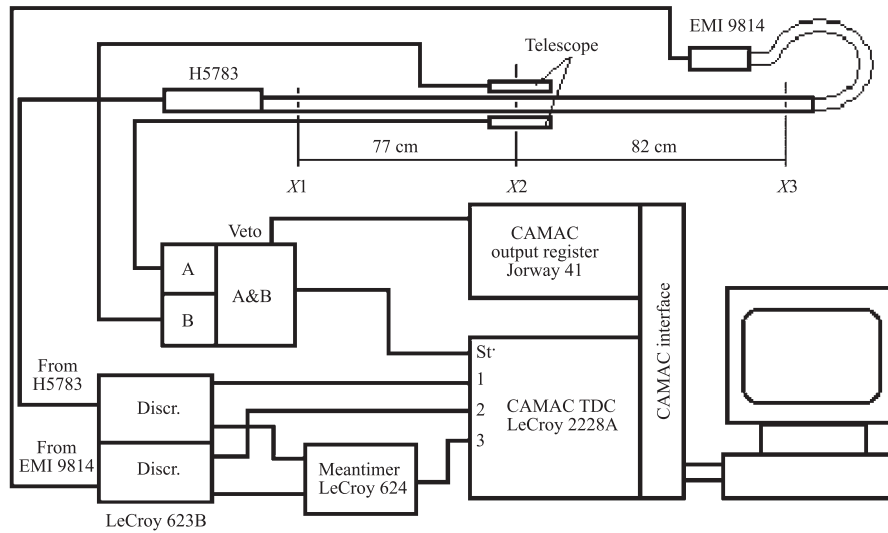


Fig. 11. Schematic representation of the setup used for measuring the MSX' counters characteristics

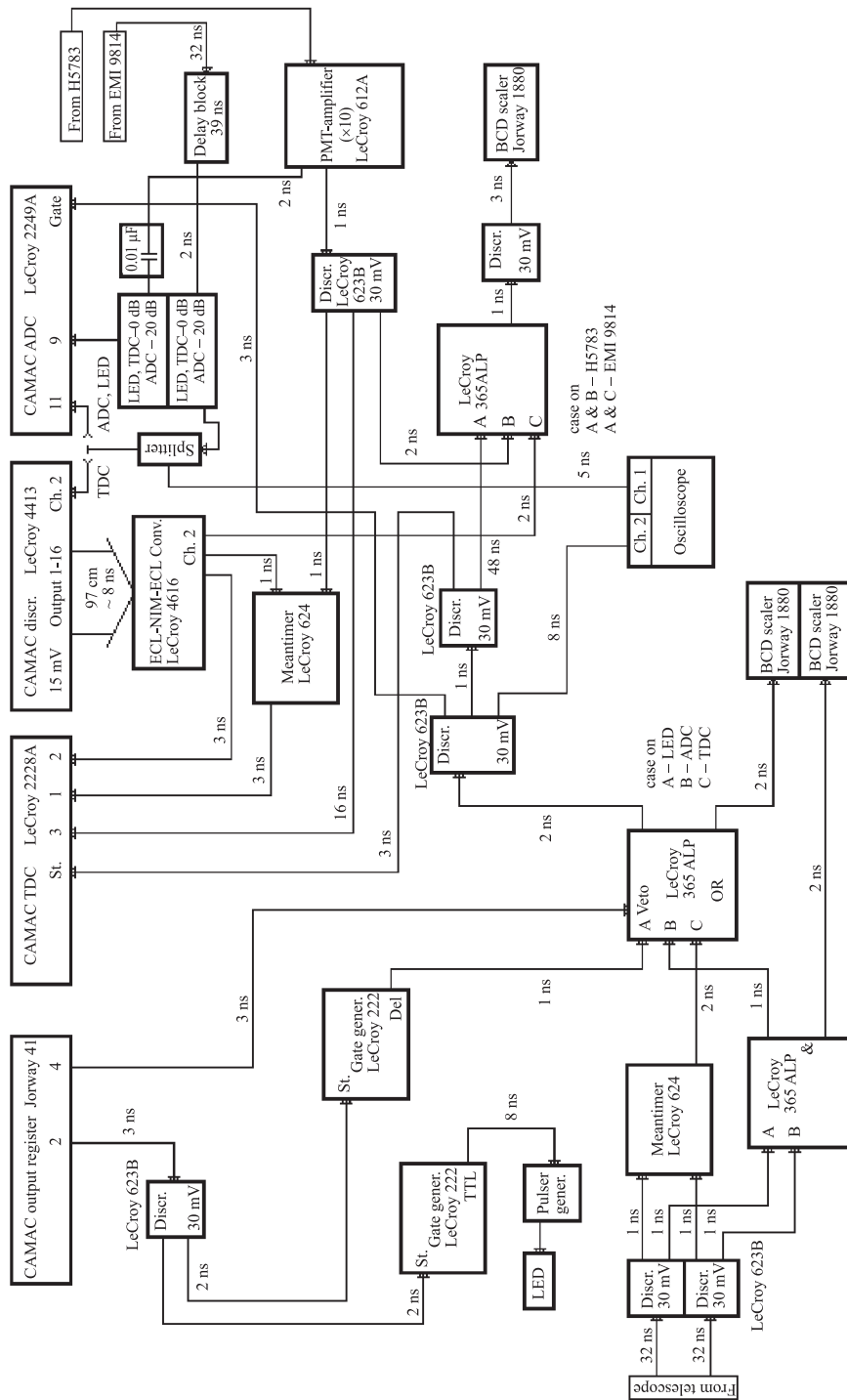


Fig. 12. Detailed schematic representation of the DAQ system

Table 1. Measured characteristics of all mixed (MSX') counters

Counter	PMT	X1			X2			X3		
		$\langle T \rangle$, ns	FWHM	σ	$\langle T \rangle$, ns	FWHM	σ	$\langle T \rangle$, ns	FWHM	σ
1	EMI	45.70	3.23	0.8	40.96	3.47	0.9	33.70	4.94	1.7
	H5783	16.00	3.70	1.1	21.60	5.70	2.1	26.60	5.50	2.05
	Meantimer	56.40	4.02	1.3	56.80	3.56	1.0	55.70	4.02	1.30
2	EMI	47.60	3.33	0.8	42.80	3.14	0.7	35.90	4.11	1.35
	H5783	15.70	4.57	1.6	20.70	4.70	1.6	26.10	5.20	1.91
	Meantimer	57.40	3.60	1.0	57.30	3.56	1.0	56.50	3.65	1.09
3	EMI	45.50	3.10	0.7	40.58	3.47	0.9	34.10	3.23	0.82
	H5783	24.40	5.10	1.8	30.10	5.68	2.1	36.70	5.86	2.22
	Meantimer	54.70	3.30	0.8	54.35	3.56	1.0	54.95	3.97	1.27
4	EMI	38.76	3.00	0.6	33.80	2.91	0.5	26.63	5.36	1.99
	H5783	23.37	4.90	1.7	28.50	5.22	1.9	33.66	5.50	2.05
	Meantimer	50.00	3.56	1.0	50.10	3.74	1.1	49.10	4.25	1.42
5	EMI	37.41	3.35	0.9	32.57	2.88	0.5	25.72	3.59	1.05
	H5783	23.06	5.00	1.8	27.90	5.17	1.8	33.06	5.78	2.19
	Meantimer	49.20	3.33	0.8	49.16	3.51	1.0	48.24	3.83	1.19
6	EMI	38.29	2.64	0.2	33.35	3.06	0.6	26.31	4.90	1.77
	H5783	23.28	4.94	1.7	28.39	4.90	1.7	33.76	5.68	2.14
	Meantimer	49.78	3.33	0.8	49.84	3.93	1.2	48.99	4.34	1.47
7	EMI	38.03	2.77	0.4	33.11	2.85	0.5	26.16	4.89	1.75
	H5783	23.64	5.22	1.9	28.43	5.59	2.1	33.78	5.08	1.85
	Meantimer	49.81	3.42	0.9	49.72	3.70	1.1	48.86	3.83	1.19
8	EMI	37.53	3.39	0.9	32.62	2.88	0.5	25.42	5.12	1.87
	H5783	22.81	4.53	1.5	27.77	5.36	1.9	32.99	5.17	1.89
	Meantimer	49.15	3.14	0.7	49.15	3.60	1.0	48.08	3.74	1.13
9	EMI	40.46	2.83	0.4	35.67	2.70	0.3	27.97	5.43	2.02
	H5783	23.81	4.85	1.7	28.73	5.04	1.8	34.13	4.39	1.50
	Meantimer	50.84	3.28	0.8	50.96	2.96	0.5	49.77	4.07	1.32
10	EMI	37.00	3.19	0.7	32.04	2.73	0.3	25.17	4.82	1.72
	H5783	22.46	4.57	1.6	27.13	4.76	1.6	32.29	4.85	1.74
	Meantimer	48.69	3.14	0.7	48.54	3.14	0.7	47.61	4.07	1.32
11	EMI	39.57	2.98	0.6	34.57	2.95	0.5	27.39	4.72	1.67
	H5783	22.51	4.76	1.6	28.69	5.59	2.1	33.74	5.36	1.99
	Meantimer	50.52	3.65	1.0	50.59	3.93	1.2	49.48	4.11	1.35
12	EMI	37.48	3.43	0.9	32.70	3.26	0.8	25.74	4.44	1.52
	H5783	23.61	4.90	1.7	28.71	5.04	1.8	33.87	5.54	2.08
	Meantimer	49.53	3.14	0.7	49.66	3.79	1.1	48.70	4.25	1.42

in the case of conventional light guide readout. However, variations of up to 1 ns were observed for the WLS fiber readout.

Variations in the mean times obtained when the outputs from dissimilar readouts are combined are shown in Fig. 10. Though statistical uncertainties increase due to the effect of the lower light-collection efficiency of the WLS fiber readout, the systematic variation in the mean times does not increase significantly.

The conclusion drawn from these measurements was that the systematic contribution from the asymmetric readout method would not significantly influence the overall uncertainty in the mean times. Though the effect on the statistical uncertainty of the lower light-collection efficiency from the WLS readout was apparent, these preliminary tests could not afford a realistic evaluation of the the total statistical uncertainty corresponding to minimally ionizing particles. Measurements of this uncertainty were made using cosmic muons and obtained $\sigma = (2.9 \pm 0.2)$ ns for similar, light guide, readouts (this result is similar to that reported for the CSX in [2]), and $\sigma = (6.3 \pm 0.5)$ ns for dissimilar readouts. Given, however, that we expected to increase the light-collection efficiency considerably by «mirroring» and by improved optical coupling, we expected that statistical uncertainties would be reduced to acceptable values when these improvements were introduced. This expectation was borne out by the tests described below.

4.2. Timing Measurements on the Final Version of the MSX' Counters. Timing measurements on the MSX' counters, constructed according to the final design parameters outlined

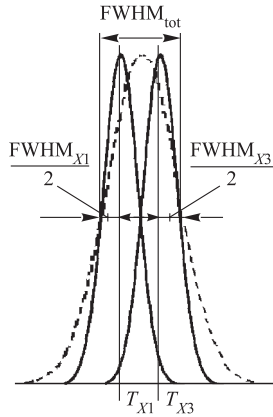


Fig. 13. The illustration of the procedure used to estimate the effect of the asymmetry systematics on the total FWHM

in section 1, were performed using cosmic muons which were selected by a scintillator «telescope», as illustrated schematically in Fig. 11 (a more detailed description of the data acquisition (DAQ) electronics is shown in Fig. 12), which consisted of $15 \times 15 \times 2$ cm scintillators, located above and below the counter being tested. The coincidence of these scintillators was used to trigger the DAQ and to start the TDCs which were stopped by the counter outputs. The contribution σ_{tr} of the trigger counters to the total timing uncertainty was measured to be 1.1 ns. Mean times were calculated by summing the TDC outputs corresponding to the two ends of the detector. They were also measured directly using a LeCroy 624 meantimer. No significant difference was found between calculated and measured mean times.

Measurements were performed at three different positions along the counters: the center (referred to as X2), a position (X1), closer to the wider end, at 77 cm from the center, and another (X3), closer to the narrower end, at 82 cm from the center. The results of these measurements are reported in Table 1, where both the full width at half-maximum (FWHM) and the standard deviation σ of both individual times and mean times are tabulated together with the mean times $\langle T \rangle$ for all MSX' counters. The standard deviation σ was corrected for the contribution of the scintillator telescope by subtracting it in quadrature: $\sigma = \sqrt{\sigma_{FWHM}^2 - \sigma_{tr}^2}$. It was noted that values of the standard deviation were generally

higher at $X3$ (the end closer to the EMI PMT) than those at other positions. This might be attributed to the presence of Cherenkov light occasioned by the passage of the cosmic muons through the light guide, which overlaps this region.

The maximum systematic variations in the mean times $\langle T \rangle$ are seen to be compatible with those measured during the preliminary tests and, in order to evaluate their effect on the overall uncertainty, the following procedure was adopted:

$$\text{FWHM}_{\text{tot}} = |\langle T_{X1} \rangle - \langle T_{X3} \rangle| + \frac{\text{FWHM}_{X1} + \text{FWHM}_{X3}}{2},$$

as illustrated in Fig. 13. The total deviation σ_{tot} was then calculated from FWHM_{tot} by dividing by 2.35. From these values (given for each counter in Table 2), it is apparent that σ_{tot} does not exceed 2.2 ns. This is quite compatible with the requirement that the resolution be sufficient to discriminate against background in conditions similar to those of Run I [2], as outlined in section 5.

Table 2. Calculated values of FWHM_{tot} , σ_{tot} , $V_{\text{light}}^{\text{eff}}$ for each MSX' counter

Counter	FWHM_{tot} , ns	σ_{tot} , ns	$V_{\text{light}}^{\text{eff}}$ (EMI), cm/ns	$V_{\text{light}}^{\text{eff}}$ (H5783), cm/ns
1	4.89	2.08	13.25	15.00
2	4.53	1.92	13.59	15.29
3	4.32	1.83	13.47	15.44
4	4.91	2.08	13.11	15.45
5	4.54	1.93	13.60	15.90
6	4.69	1.99	13.27	15.17
7	4.58	1.94	13.40	15.68
8	4.51	1.92	13.13	15.62
9	4.87	2.07	12.89	15.60
10	4.69	1.99	13.44	16.17
11	5.13	2.18	13.05	15.54
12	4.98	2.11	13.54	15.50

5. INSTALLATION AND OPERATION

Teflon guides and steel runners were then fixed to each counter so they could be slid into position along steel guides fixed to their corresponding drift chamber assemblies. The disposition of counters, power supply and readout at CDF are shown schematically in Fig. 14.

Power is supplied to the EMI-type PMTs by power supplies, known as «Gamma Boxes» (supplied by Gamma High Voltage Research Inc., USA) located in the «Counting Room», via 40-channel distribution units, known as «Pisa Boxes» (originally built at the University of Pisa) located close to the detector, through RG58 HV cables. The Hamamatsu PMTs

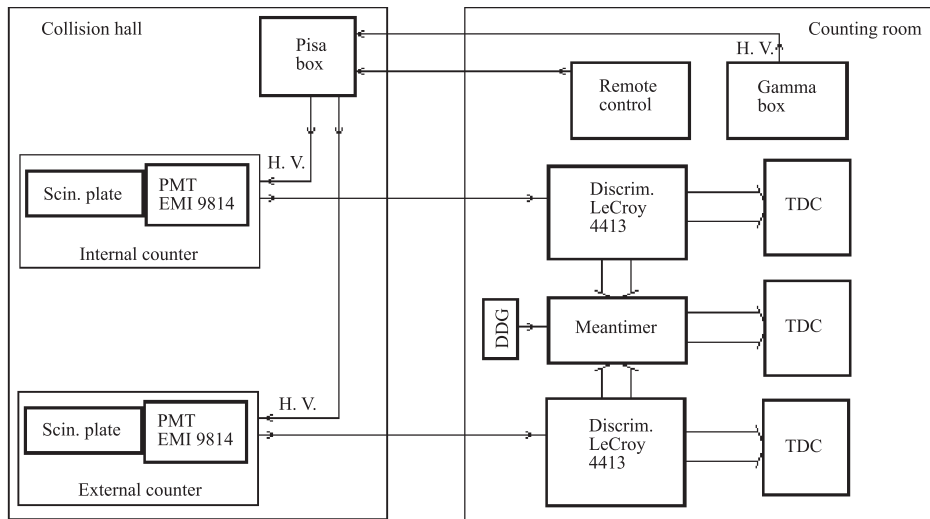


Fig. 14. The disposition of CSX counters (including «miniskirt» counters), high-voltage power supply, and signal readout from the «miniskirt» counters

received their power from supply and distribution units known as CCUs [5], located close to the detector. All the power distribution is controlled and monitored by software developed *ad hoc* [6]. This software allows for channel-by-channel control and monitoring, both manually and automatically, on a regularly scheduled basis.

Analog signals from the EMI-type PMTs are all routed to LeCroy 4413 discriminators, located in the counting room, through 67-m RG58 cables. All discriminator thresholds are set to their minimum values (15 mV). Discriminator outputs were routed both to meantimer units (located close to the discriminators) and to TDCs via 12.2-m twist and flat cable. Meantimer outputs are also routed to TDCs via the same twist and flat cables.

Presently, only three sections of standard MSX counters (i. e., with conventional light guide readout on both sides) are installed. The remaining section and the four wedges with the MSX' counters will probably be installed during a forthcoming shutdown.

Acknowledgements. The authors would like to thank A. Sissakian for his leadership and support, W. Bowman for his valuable help during counters assembling, and A. Semenov for numerous fruitful discussions.

REFERENCES

1. *The CDF II collaboration.* The CDF II Detector Technical Design Report. Fermilab-Pub-96/390-E. 1996.
2. *Giromini P. et al.* The Central Muon Extension Scintillators (CSX). CDF Note 3898. 1996.

3. *Cabrera S. et al.* Making the Most of Aging Scintillator // Nucl. Instr. Meth. A. 2000. V.453. P.245–248.
4. *Bellamy E.H. et al.* Absolute Calibration and Monitoring of a Spectrometric Channel Using a Photomultiplier // Nucl. Instr. Meth. A. 1994. V. 339. P. 468–476.
5. *Bromberg C. (for the CDF collaboration).* Gain and Threshold Control of Scintillation Counters in the CDF Muon Upgrade for Run II // Intern. J. Mod. Phys. A. 2001. V. 16. Suppl. 1C. P. 1143–1146.
6. *Pukhov O. et al.* Automatization of the Muon Scintillator System Power Supply at CDF II. CDF Note 5949. 2002.

Received on November 4, 2002.